Published in final edited form as:
Cancer Biol Ther. 2010 May ; 9(10): 778–790.

Oral delivery of PND-1186 FAK inhibitor decreases tumor growth and spontaneous breast to lung metastasis in pre-clinical models

Colin Walsh[1,*], **Isabelle Tanjoni**[1,*], **Sean Uryu**[1], **Alok Tomar**[1], **Ju-Ock Nam**[1], **Hong Luo**[2], **Angelica Phillips**[2], **Neela Patel**[2], **Cheni Kwok**[2], **Gerald McMahon**[2], **Dwayne G. Stupack**[1,#], and **David D. Schlaepfer**[1,#]

[1]Departments of Reproductive Medicine and Pathology, University of California San Diego Moores Cancer Center, La Jolla, CA 92093

[2]Poniard Pharmaceuticals Inc., South San Francisco, CA 94080

Abstract

Tumor metastasis is a leading cause of cancer-related death. Focal adhesion kinase (FAK) is a cytoplasmic tyrosine kinase recruited to integrin-mediated matrix attachment sites where FAK activity is implicated in the control of cell survival, migration, and invasion. Although genetic studies support the importance of FAK activity in promoting tumor progression, it remains unclear whether pharmacological FAK inhibition prevents tumor metastasis. Here, we show that the FAK inhibitor PND-1186 blocks FAK Tyr-397 phosphorylation *in vivo* and exhibits anti-tumor efficacy in orthotopic breast carcinoma mouse tumor models. PND-1186 (100 mg/kg intraperitoneal, i.p.) showed promising pharmacokinetics (PK) and inhibited tumor FAK Tyr-397 phosphorylation for 12 hours. Oral administration of 150 mg/kg PND-1186 gave a more sustained PK profile verses i.p., and when given twice daily, PND-1186 significantly inhibited sygeneic murine 4T1 orthotopic breast carcinoma tumor growth and spontaneous metastasis to lungs. Moreover, low-level 0.5 mg/ml PND-1186 *ad libitum* administration in drinking water prevented oncogenic *KRAS*- and *BRAF*-stimulated MDA-MB-231 breast carcinoma tumor growth and metastasis with inhibition of tumoral FAK and p130Cas phosphorylation. Although PND-1186 was not cytotoxic to cells in adherent culture, tumors from animals receiving PND-1186 exhibited increased TUNEL staining, decreased leukocyte infiltrate and reduced tumor-associated splenomegaly. *In vitro*, PND-1186 reduced tumor necrosis factor-α triggered interleukin-6 cytokine expression, indicating that FAK inhibition may impact tumor progression via effects on both tumor and stromal cells. As oral administration of PND-1186 also decreased experimental tumor metastasis, PND-1186 may therefore be useful clinically to curb breast tumor progression.

Keywords

FAK; apoptosis; tumor growth; tumor metastasis; inflammation

Address correspondence to: David D. Schlaepfer, Ph.D., University of California San Diego, Moores Cancer Center, Department of Reproductive Medicine, 0803, 3855 Health Sciences Dr., La Jolla, CA 92093, Phone: (858) 822-3444, dschlaepfer@ucsd.edu.
[*]both authors contributed equally to this study
[#]co-corresponding authors

Conflicts of Interest Disclosure

Hong Luo, Angelica Phillips, Cheni Kwok, Neela Patel, and Gerald McMahon are associated with Poniard Pharmaceuticals Inc. No other conflicts of interest.

Introduction

Breast cancer is the second highest cause of cancer-related death and the most frequent cancer diagnosed in women. A primary complication of breast cancer is metastasis1. While the five-year breast cancer survival rate for women with localized breast cancer is 98%, this drops to 27% for women with distant organ metastasis2, 3. New treatments are needed to combat metastatic disease.

Focal adhesion kinase (FAK) is a cytoplasmic protein-tyrosine kinase that associates with both integrins and growth factor receptors to control cell motility, invasion, and survival4, 5. FAK is over expressed in invasive or metastatic breast cancer 6–10 due in part to gene amplification at 8q2411 and elevated FAK levels are correlated with a poor prognosis8, 10, 12. Elevated FAK expression can also be an early event in breast cancer progression13, 14. FAK acts as both a signaling kinase and cell adhesion-associated scaffold within tumor cells to coordinate the positional recruitment and phosphorylation of various cytoskeletal-associated proteins such as p130Cas4, 15. The molecular mechanisms through which FAK has been linked to cancer progression are by promoting angiogenesis16, enhanced cell proliferation and survival17, 18, and by facilitating a switch to an invasive cell phenotype19–21.

Previously, we demonstrated that FAK knockdown reduced the metastatic potential of 4T1 murine breast cancer cells and increased the survival of tumor-bearing Balb/c mice22. Re-expression of wild-type, but not kinase-dead FAK, in 4T1 FAK knockdown cells restored spontaneous breast to lung metastasis, providing the first genetic proof that FAK catalytic activity facilitates metastatic breast cancer progression22. Additionally, dominant-negative approaches to limit FAK activity via expression of the FAK C-terminal domain prevented primary syngeneic rat breast carcinoma tumor growth and experimental metastasis23. As integrin-mediated activation of FAK facilitates the experimental extravasation of mouse mammary carcinoma cells in the lung24, and knockdown of FAK results in reduced proliferation and increased mammary carcinoma cell apoptosis10, there is much interest in determining whether small molecule inhibitors of FAK activity will block breast tumor growth and metastasis.

ATP-competitive small molecule inhibitors to FAK have been developed by Novartis (TAE-226) and Pfizer (PF-573,228 and PF-562,271)25–27. TAE-226 is also a high-affinity inhibitor of insulin-like growth factor receptor28. TAE-226 can prevent glioma tumor growth in mice27, 28 and in combination with docetaxel, TAE-226 can facilitate xenotropic ovarian carcinoma tumor regression29. PF-573,228 and PF-562,271 are highly selective for FAK and the related Pyk2 kinase. PF-562,271 oral administration reduces the growth of lung, prostate, pancreatic, glioma, colon, and breast subcutaneous human tumor xenografts in nude mice26 and inhibits the growth of castration-resistant cancer in a transgenic adenocarcinoma of the mouse prostate (TRAMP) model30. Based upon the broad anti-tumor activity of PF-562,271, it has entered clinical trials31. However to date, no pre-clinical models have investigated the effects of FAK inhibition with regard to blocking breast cancer metastasis.

Herein, we extend the characterization of a reversible small molecule inhibitor of FAK activity, PND-118632. We show that PND-1186 administration inhibits FAK and downstream substrate p130Cas tyrosine phosphorylation in orthotopic breast tumors. Oral PND-1186 dosing provided significant anti-tumor and anti-metastatic effects in two different (4T1 and MDA-MB-231) orthotopic breast carcinoma mouse tumor models without animal morbidity, death or weight loss. PND-1186 significantly decreased tumor-associated inflammatory cell infiltration and splenomegaly in mice with syngeneic 4T1

tumors, suggesting PND-1186 can reduce tumor-associated inflammation. Thus, PND-1186 may therefore be useful clinically to curb multiple aspects of breast carcinoma tumor progression.

Results

Pharmacokinetic evaluation of PND-1186

PND-1186 is a selective small molecule inhibitor of FAK with an IC_{50} of ~0.1 μM in cultured breast carcinoma cells as determined by anti-phospho-specific immunoblotting to the major FAK autophosphorylation site, Tyr-39732. PND-1186 prevents cell motility in a dose-dependent fashion (0.1 to 1.0 μM), yet 1.0 μM PND-1186 has limited inhibitory effects on adherent cell proliferation. Importantly, we found that low-level 0.1 μM PND-1186 selectively promotes carcinoma cell apoptosis under three-dimensional culture conditions32. Moreover, PND-1186 triggered 4T1 apoptosis when grown as subcutaneous tumors. Orthotopic implantation of 4T1 cells into the breast fat pad is a model of late-stage breast cancer where spontaneous breast to lung metastasis occurs rapidly33. Herein, we test the hypothesis that PND-1186 may prevent breast carcinoma tumor progression.

As a first step, PND-1186 pharmacokinetics (PK) were determined in Balb/c mice following intravenous (i.v.), intraperitoneal (i.p.), and oral (p.o.) administration (Table I). PND-1186 displayed a multi-exponential decay with a terminal half life ($t_{1/2}$) of 1.72 hours after i.v. injection. Following i.p. and p.o. dosing, PND-1186 was rapidly absorbed (Table 1, Figure 1A and 2A) with terminal half lives ($t_{1/2}$) of 2.15 to 2.65 h, and bioavailability (%F) from 14.8 to 42.2% (Table 1). PND-1186 bioavailability was greater upon intraperitoneal versus oral dosing (Table I). PND-1186 plasma concentrations, maximum concentration (C_{max}), and the area under the plasma concentration-time curve (AUC) from time zero to infinity (0-inf) increased in a linear fashion as a function of dose (data not shown).

PND-1186 inhibits FAK and p130Cas tyrosine phosphorylation *in vivo*

PND-1186 inhibits FAK Tyr-397 phosphorylation in adherent and suspended 4T1 cells, however p130Cas tyrosine phosphorylation is selectively inhibited by PND-1186 treatment in suspended cells32. To determine if PND-1186 affects FAK and p130Cas in solid tumors, subcutaneous 4T1 breast carcinoma tumors were established and a single i.p. injection of vehicle (50% PEG400 in PBS) or PND-1186 was administered (Fig. 1A and B). For 100 mg/kg PND-1186, maximal plasma levels (117 μM) were reached within 30 min and maximal PND-1186 in tumors (16.1 μg/g) was achieved within 1 h and maintained up to 12 h (with plasma levels at 1.1 μM at 12 h). 100 mg/kg PND-1186 resulted in sustained inhibition (>60%) of tumor FAK Tyr-397 phosphorylation (pY397 FAK) for 12 h (Fig. 1C and D) and significantly reduced p130Cas Tyr-410 phosphorylation (pY410Cas) by 3 h (Fig. 1E, F, and Supplemental Figure 1). Similar results were obtained when using phospho-specific antibodies to pTyr-249 of p130Cas (data not shown). For 30 mg/kg PND-1186, maximal plasma levels (35 μM) were reached within 15 min and maximal PND-1186 in tumors (0.75 μg/g) was achieved within 1 h (Fig. 1B). This was sufficient to inhibit FAK pY397 phosphorylation for 3 to 6 h after which time tumor PND-1186 levels fell to 0.04 μg/g by 12 h (with plasma levels at 0.1 μM) at which point tumor FAK pY397 phosphorylation was not significantly inhibited (Supplemental Figure 2). These results show that PND-1186 inhibits FAK and p130Cas tyrosine phosphorylation in tumors in a dose-dependent manner *in vivo* and that plasma levels at or above 1 μM are sufficient to promote tumor-associated FAK inhibition.

Orally-dosed PND-1186 inhibits 4T1 orthotopic tumor growth associated with increased tumor apoptosis

Oral bioavailability of PND-1186 in water is less than when administered intraperitoneally (Table I). As 150 mg/kg oral dose of PND-1186 resulted in maximal plasma level of ~14 μM by 4 h and a sustained plasma level of PND-1186 above 3 μM for 12 h (Fig. 2A), this oral (p.o) twice-daily (b.i.d.) dose was tested for anti-tumor efficacy using orthotopic implanted mCherry-fluorescent 4T1 tumor cells. By Day 7, 150 mg/kg PND-1186 significantly reduced tumor volume compared to vehicle control (Fig. 2B). By 16 days, 150 mg/kg PND-1186 reduced final tumor volume 3-fold (Fig. 2B and C) and final tumor weight was reduced 3.1-fold (Fig. 2D) compared to vehicle control without affects on total body weight (Supplemental Figure 3). Analyses of primary breast fat pad 4T1 tumors revealed a high number of blood vessels as detected by anti-CD31 staining (data not shown). Although previous studies with lung carcinoma xenografts showed reduced tumor microvessel density after PF-562,271 administration26, no major vascular differences were observed in PND-1186-treated 4T1 orthotopic tumors as determined by anti-CD31 staining (data not shown). To determine a potential molecular mechanism to account for the smaller size of PND-1186-treated 4T1 tumors, medial sections were analyzed by deoxynucleotidyl transferase dUTP nick end labeling (TUNEL) (Fig. 2E and F). Mice administered PND-1186 exhibited 2.8-fold increased TUNEL staining in breast fat pad tumors compared to vehicle-treated controls. This result suggests that increased tumor cell apoptosis could be one mechanism responsible for the inhibition of tumor growth by PND-1186.

PND-1186 reduces tumor-associated inflammation

In the tumor microenvironment, inflammation can facilitate tumor progression by promoting cell proliferation, survival, and metastasis34, 35. Aggressive breast cancer is characterized by primary tumor leukocyte infiltration36. As 4T1 tumors in Balb/c mice are known to trigger a leukemoid reaction37, 4T1 tumor sections were analyzed for CD45 staining, a common marker present on macrophages and other hematopoietic cells (Fig. 3A). In untreated (data not shown) and vehicle-treated mice, there was abundant number of CD45-positive cells present within 4T1 primary tumors (Fig. 3B and Supplemental Figure 4). Mice treated with 150 mg/kg PND-1186 exhibited a 2.8-fold decrease in CD45 tumor-associated staining (Fig. 3A and B) and this is supportive of reduced immune cell infiltration into 4T1 tumors upon PND-1186 treatment.

To determine if this was localized or a systemic response, spleen size was analyzed in normal Balb/c mice or tumor-bearing mice treated with vehicle or PND-1186 (Fig. 3C and D). It is known that 4T1 tumor growth is associated with increased spleen size, or splenomegaly-associated inflammation37. Spleens from vehicle-treated mice weighed >2-fold more than PND-1186-treated mice (Fig. 3D). Notably, spleens from PND-1186-treated mice were healthy and indistinguishable from non-treated, non-tumor bearing mice (Fig. 3D). As splenomegaly is due in part to increased inflammatory cytokine production, 4T1 cells in culture were stimulated by tumor necrosis factor-α (TNFα) addition and interleukin-6 (IL-6) cytokine production was measured by an enzyme-linked immunosorbent assay (ELISA) (Fig. 3E). TNFα triggered >4-fold increase in 4T1 IL-6 production and PND-1186 addition (0.25 to 1.0 μM) inhibited IL-6 release in a dose-dependent manner. IL-6 is pleiotropic cytokine involved in inflammation and breast cancer progression38 and our results support the notion that anti-inflammatory effects of PND-1186 treatment may act to limit 4T1 tumor progression.

PND-1186 inhibits spontaneous 4T1 breast tumor metastasis to lung

4T1 tumors are used a model of late-stage breast cancer progression33. 4T1 cells implanted into the breast fat pad will intravasate into the blood circulation and form pulmonary

metastases within 7 to 10 days39. As PND-1186 inhibits both 4T1 tumor growth and associated inflammation, the metastatic distribution of mCherry-fluorescent 4T1 cells was determined after orthotopic breast fat pad injection and PND-1186 (150 mg/kg p.o., b.i.d.) treatment for 15 days (Fig. 4A). Direct visualization of mCherry fluorescence from dorsal and ventral lung images was quantified, the number of lung metastases counted, and distributions grouped as negligible, moderate, or high (Fig. 4B). For vehicle control mice, the majority had moderate and high lung metastatic burden (7/12) whereas in PND-1186 mice, the majority had negligible lung metastases (7/12) and no mice with a high metastatic burden. These findings were confirmed by hematoxylin and eosin (H&E) staining of lung sections that showed detectable 4T1 lung metastases in control but not PND-1186-treated mice (Fig. 4C). The findings are the first to show that a small molecule inhibitor to FAK can interrupt the processes of spontaneous breast cancer metastasis.

Ad libitum PND-1186 administration inhibits 4T1 tumor growth and metastasis

As studies with PF-562,271 revealed that continuous low dose administration was equally effective as 50 mg/kg twice daily dosing in preventing xenograft tumor growth26, we investigated whether low dose PND-1186 was effective in preventing 4T1 orthotopic tumor progression (Fig. 5). PND-1186 is water soluble (>20 mg/ml) and we found that mice would accept 0.5 mg/ml PND-1186 in 5% sucrose in lieu of drinking water. Mice were allowed to self-dose PND-1186 *ad libitum* and control mice were provided 5% sucrose as drinking water. PK evaluation revealed mean PND-1186 plasma and tumor concentrations of 1.2 μM and 521.7 ng/g, respectively after 7 days. Mice showed no signs of toxicity or weight loss with *ad libitum* PND-1186 administration.

To determine the effects on tumor growth, a*d libitum* PND-1186 administration was initiated 48 h after mCherry-4T1 orthotopic tumor implantation. By Day 13, tumor size was significantly different as determined by caliper measurements (Fig. 5A) and by Day 22, PND-1186 administration inhibited final tumor mass >1.8 fold (Fig. 5B) without toxicity or weight loss. In immunoblotting analyses of primary 4T1 tumors, a*d libitum* PND-1186 administration was sufficient to inhibit both FAK pY397 and p130Cas pY410 phosphorylation (Fig. 5C and D). Ad libitum PND-1186 also inhibited pY118 paxillin phosphorylation but not pY416 Src nor pY402 Pyk2, pS473 Akt, or pT308 Akt phosphorylation in tumors (Supplemental Figure 5). Spleen comparisons revealed that a*d libitum* PND-1186 treated mice were of normal size whereas control mice had enlarged spleens (data not shown). Control mice receiving 5% sucrose exhibited a moderate to high lung metastatic burden (9/11) whereas the majority of *ad libitum* PND-1186 mice had a neglible to moderate lung metastatic burden (13/15) (Fig. 5E). Taken together, the results support the conclusion that low level PND-1186 administration was efficacious in slowing 4T1 tumor progression.

PND-1186 administration inhibits MDA-MB-231 orthotopic tumor growth and metastasis

To extend the 4T1 findings to human breast carcinoma, MDA-MB-231 cells containing activating mutations in K-Ras and B-Raf40 were implanted in the breast fat pad of severe combined immunodeficiency (SCID) mice. After 12 days, when tumors became palpable, 0.5 mg/ml PND-1186 or control 5% sucrose was provided *ad libitum* as drinking water (Fig. 6). By experimental Day 27 (15 days of PND-1186 administration), control tumors were significantly larger as determined by caliper measurements (Fig. 6A) and at Day 70, *ad libitum* PND-1186 administration resulted in a >5- fold decrease in final tumor weight (Fig. 6B and C). Low level PND-1186 treatment was sufficient to significantly reduce FAK pY397 phosphorylation in MDA-MB-231 tumors (Fig. 6D). To determine the effect on spontaneous MDA-MB-231 metastasis, lungs from SCID mice were sectioned, H&E-stained, and micro-metastases enumerated (Fig. 6E). Control mice exhibited detectable

metastasis and PND-1186 *ad libitum* treatment reduced the number of metastatic lung lesions >3.5-fold (Figure 6F).

As PND-1186 treatment reduces primary tumor size which can affect a number of factors influencing tumor cell metastasis41, experimental metastasis assays were performed by tail vein injection of dsRed fluorescent protein-expressing MDA-MB-231 cells. Mice were pre-administered 150 mg/kg PND-1186 or water (vehicle) p.o. and the accumulation or lodging of tumor cells within lung capillaries after 1 or 6 h was quantified by fluorescent imaging (Fig. 7A and B). At both 1 and 6 h, PND-1186 significantly inhibited the accumulation of tumor cells in the lungs. As blood plasma levels of PND-1186 are likely above 1 μM in the experimental metastasis assay, MDA-MB-231 apoptosis was analyzed *in vitro* by incubating cells in suspension with PND-1186. As determined by annexin V binding and quantified by flow cytometry, concentrations up to 10 μM PND-1186 did not promote MDA-MB-231 apoptosis within 6 h (Fig. 7C). The molecular mechanism of how PND-1186 reduces experimental metastasis remains to be determined. Taken together, these results show that oral PND-1186 administration decreases FAK tyrosine phosphorylation *in vivo* resulting in robust anti-tumor and anti-metastatic activity using two different orthotopic breast carcinoma models.

Discussion

Increased FAK expression and activity are associated with breast cancer progression and a poor prognosis6¯10. Previously, we demonstrated that FAK knockdown reduced the metastatic potential of 4T1 murine breast cancer cells and increased the survival of tumor-bearing Balb/c mice22. Re-expression of wild-type, but not kinase-dead FAK, in 4T1 FAK knockdown cells restored spontaneous breast to lung metastasis, providing the first genetic proof that FAK catalytic activity facilitates metastatic breast cancer progression22. Recent studies have confirmed the importance of FAK in promoting breast carcinoma tumor progression through analysis of knockout mice10, 17, 18, 42, but this work does not directly address the role of intrinsic FAK activity as opposed to the role of FAK as an integrin- or nuclear-associated scaffolding protein43, 44. Herein, we provide evidence from 4T1 and MDA-MB-231 breast carcinoma models that a small molecular inhibitor of FAK (PND-1186) acts as an effective anti-tumor and anti-metastatic drug to limit breast cancer progression.

Pharmacokinetic analyses revealed that blood plasma levels of 1 μM PND-1186 were sufficient to facilitate the inhibition of FAK and p130Cas tyrosine phosphorylation within tumors implanted subcutaneously (Fig. 1) or orthotopically in mouse breast fat pads (Fig. 5). This could be achieved and maintained for 12 h by oral administration of 150 mg/kg PND-1186 (Fig. 2) and also by 0.5 mg/ml *ab libitum* administration of PND-1186 in the drinking water (Table I). Statistically significant inhibition of tumor growth occurred 7 to 10 days following the initiation of PND-1186 administration and final tumor weight was reduced 3.1-fold (Fig. 2) or >5-fold (Fig. 6) in 4T1 or MDA-MB-231 models, respectively. In contrast to xenotropic subcutaneous tumor studies with Pfizer PF562,27126, we did not observe effects on 4T1 tumor micro-vascular density. One might argue that aggressive 4T1 tumor growth, which secretes many inflammatory and angiogenic growth factors, could be sufficient to override anti-angiogenic effects of FAK inhibition44.

However, PND-1186 administration increased 4T1 tumor-associated apoptotic TUNEL staining that could account for PND-1186 inhibition of tumor growth (Fig. 2). Notably, whereas PND-1186 has only limited effects on adherent 4T1 cell proliferation, PND-1186 inhibition of FAK and p130Cas tyrosine phosphorylation was associated with increased 4T1 cell apoptosis grown as suspended spheroids, in soft agar, or in three-dimensional (3D)

Matrigel culture conditions32. We speculate that this reflects a direct role for FAK-mediated p130Cas tyrosine phosphorylation as PND-1186 does not inhibit Src activity in either adherent or suspended 4T1 cells32. In vivo, we found that PND-1186 inhibited p130Cas and paxillin, but not Src or Pyk2 tyrosine phosphorylation within orthotopic tumors (Fig. 5 and Supplemental Fig. 5). Importantly, PND-1186 did not inhibit Akt phosphorylation and this supports the notion that a potential FAK-p130Cas signaling linkage may promote 3D cell survival in a non-canonical manner. FAK expression is needed for the survival of various human breast cancer cells carrying clinically prevalent oncogenic mutations10 and our results support the hypothesis that this is likely associated with FAK-mediated p130Cas phosphorylation. Notably, MDA-MB-231 cells carry activating mutations in *KRAS* and *BRAF*40. Although a recent publication implicated oncogenic Ras-induced tyrosine dephosphorylation of FAK in facilitating Ras-induced cell motility and tumor metastasis45, our results showing that PND-1186 inhibits both FAK pY397 phosphorylation and orthotopic-initiated MDA-MB-231 pulmonary metastatic burden (Fig. 6) are incongruous with the preceding study.

The molecular mechanisms linking FAK signaling to tumor progression are varied and include the regulation of angiogenesis, the facilitation of an invasive cell phenotype, and the enhancement of cell survival 43, 46. Our studies with 4T1 cells in immunocompetent Balb/c mice also have uncovered another means through which FAK may affect tumor progression; via the regulation of tumor-associated inflammation. PND-1186 significantly decreased inflammatory cell infiltration within tumors and prevented splenomegaly that accompanied 4T1 tumor progression (Fig. 3). The release of inflammatory cytokines from growing tumors contribute to inflammation34 and we found that PND-1186 prevented TNFα-stimulated IL-6 production in a dose-dependent manner (Fig. 3). Although the processes accompanying inflammation can promote tumor metastasis47, elevated IL-6 levels are a poor prognostic index for breast cancer48, and FAK is important for TNFα-stimulated IL-6 production in other cell types49, it remains to be determined whether FAK-mediated IL-6 production enables tumor metastasis.

One process that contributes to cell metastasis is intrinsic tumor cell motility41. Pfizer PF-573,228 prevented prostate carcinoma cell motility in vitro25 and PND-1186 inhibited 4T1 cell movement in a dose-dependent manner32. Importantly, PND-1186 administration significantly reduced pulmonary metastatic burden in both the 4T1 and MDA-MB-231 tumor models (Fig. 4 and Fig. 6). Although changes in cell motility can affect the escape-release of tumor cells from the primary tumor site, experimental metastasis assays performed by tail vein injection of tumor cells measure events post tumor cell intravasation into the bloodstream. Pre-administration of PND-1186 to mice reduced experimental metastasis as measured by the lodging-accumulation of fluorescent MDA-MB-231 cells in the lungs from 1 to 6 h (Fig. 7). Our findings are consistent with the inhibition of FAK expression within 4T1 or MDA-MB-231 cells in preventing breast to lung metastasis20, 22. However, the molecular mechanism to account for the inhibition of experimental metastasis remains unclear as we did not detect increased apoptosis within 6 h and our analyses likely precede trans-endothelial tumor cell extravasation10, 50 or potential effects on metastatic cell proliferation24. Nevertheless, this result suggests that FAK inhibition can prevent tumor metastasis independent of effects on primary tumor growth.

In summary, our results with PND-1186 support a novel role for FAK signaling in promoting the long-term survival of tumor cells in three-dimensional environments. Moreover, our results support varied roles for FAK signaling in promoting tumor progression. As PND-1186 has low intrinsic toxicity to mice, there is significant merit for testing PND-1186 as an anti-cancer therapy in the clinic.

Materials and Methods

Reagents and cells

Antibodies to FAK were from Millipore. Site and phospho-specific antibodies to pY249 p130Cas, pY410 p130Cas, pY416 Src, and antibodies to c-Src were from Cell Signaling Technology. Anti-pY397 FAK was from Invitrogen and antibodies to p130Cas were from Santa Cruz Biotechnology. 4T1 murine mammary carcinoma cells and MDA-MB-231 human breast carcinoma cells were from American Type Culture Collection. Cells were cultured in Dulbecco's modified Eagle's medium supplemented with 10% fetal bovine serum (FBS), 1 mM non-essential amino acids, 2 mM glutamine, 100 U/ml penicillin, and 100 μg/ml streptomycin. mCherry-labeled 4T1 and MDA-MB-231 cells were created as described32. Selection of highly metastatic mCherry 4T1 cells was performed by isolation and expansion of cells from lung metastases. Briefly, mCherry-4T1 cells were harvested and injected into the T4 mammary fat pad of 8–10 week female Balb/c mice. After 4 weeks the lungs were removed, dissociated into single cells using elastase and collagenase treatments, and then cultured with 60 μM of 6-thioguanine (Sigma) for 2 weeks to select for 4T1 cells 39. A population of mCherry-4T1 cells (4T1-L) was obtained by fluorescence-activated cell sorting (FACS), treated with ciprofloxacin (10 μg/ml), verified to be mycoplasma-negative via polymerase chain reaction (Stratagene), and re-verified to establish spontaneous lung metastatic colonies within 10 days after breast fat pad injection.

Immunoblotting

Protein extracts of cells were made using lysis buffer containing 1% Triton X-100, 1% sodium deoxycholate, and 0.1% SDS and were separated by 4–12% SDS-PAGE and sequential immunoblotting performed as described22. Relative expression levels and phospho-specific antibody reactivity were measured by densitometry analyses of blots using Image J (Version 1.42q). Inhibition of FAK and p130Cas tyrosine phosphorylation was quantified by calculating the ratio of pY397 FAK protein to total FAK. Similar analyses were performed for p130Cas using pY410 p130Cas and total p130Cas blot data.

Immunohistochemistry

For the detection of apoptosis, sections (7 μm) were analyzed using a terminal deoxynucleotidyl transferase dUTP nick end labeling (TUNEL) kit (Roche). For CD45 staining, sections (7 μm) were fixed in 4% paraformaldhyde, rinsed in PBS, and blocked with a solution of PBS containing 5% BSA, 1% goat serum and 0.1 % Triton X. FITC-conjugated anti-CD45 antibodies (Invitrogen) at 1 μg/ml in 5% BSA and PBS were incubated for 2 hours. FITC-conjugated IgG2b isotype antibodies (Invitrogen) at the same concentration were used as a negative control. Cell nuclei were visualized by incubation with 1:25,000 dilution of Heochst 33342 (Invitrogen). Images were sequentially captured at 40× (UPLFL objective, 1.3 NA; Olympus) using a monochrome charge-coupled camera (ORCA ER; Hamamatsu), an inverted microscope (IX51; Olympus), and Slidebook software (v5.0, Intelligent Imaging). Images were pseudo-colored, overlaid, and merged using Photoshop CS3 (Adobe). Fluorescence quantitation was performed using Image J (v1.43).

IL-6 ELISA

Two million 4T1 cells were plated and allowed to spread for 4 h in 10% FBS after which time, DMSO (control) or the indicated concentration of PND-1186 was added. After 1 h, recombinant tumor necrosis factor-α (TNFα) (eBioScience) was added (10 ng/ml) and after 24 h, IL-6 levels in conditioned media were measured using anti-mouse IL-6 ELISA kit (eBioScience).

Mouse studies

Female BALB/c, BALB/c SCID, or nude (Nude-Foxn1^{nu}) mice were used for in vivo studies. Mice were from Harlan Laboratories (Indianapolis, IN) and housed in pathogen-free conditions, according to the guidelines of the Association for the Assessment and Accreditation for Laboratory Animal Care, International. Studies were performed with approved institutional animal care and use protocols. No body weight loss or morbidity was associated with the study protocols.

Pharmacokinetic (PK) evaluation of PND-1186

For intravenous (i.v.) injections, mice were given vehicle or 2 mg/kg PND-1186 in 10% DMSO, 10% Tween 80, and 80% water. For intraperitoneal (i.p.) injections, mice were given 30 or 100 mg/kg PND-1186 in 50% PEG400 in PBS. For oral (p.o.) administration, mice were given 150 mg/kg PND-1186 in water. Blood samples were collected via terminal heart puncture at 0.5, 1, 2, 4, 8, 12, 24 and 48 h for p.o. administration and 0.083, 0.25, 0.5, 1, 2, 4, 8, 12, 24 and 48 h for i.p. and i.v. administration. 3 mice per time point were used. For *ad libitum* administration, blood samples were collected after 7 days using five mice per group. Samples were collected in tubes containing 0.05 ml 0.5M EDTA, centrifuged at 900xg for 15 min at room temperature, and the plasma collected. PND-1186 content was determined by high-performance liquid chromatography (HPLC) and mass spectroscopy analyses (see Supplemental Methods).

Pharmacodynamic (PD) evaluation of PND-1186

4T1 cells were injected in the flank of Balb/c mice and allowed to grow as tumors (300–400 mm^3) for 10 days. Vehicle (50% PEG400 in PBS), 30 or 100 mg/kg PND-1186 were i.p. injected and mice were sacrificed at 1, 3, 6 and 12 hours. Five mice were used per group. Tumors were resected and homogenized using a Pro 200 tissue homogenizer (Pro Scientific) in lysis buffer containing 1% Triton-X 100, 50 mM Hepes pH 7.4, 150mM NaCl, 10% Glycerol, 1.5 mM $MgCl_2$, 1 mM EGTA, 10 mM sodium pyrophosphate, 100 mM NaF, 1 mM sodium orthovanadate, 10 μg/ml leupeptin, 10 μg/ml aprotinin. Protein concentration in lysates was determined using the micro bicinchoninic acid kit (Thermo). Equal protein lysates were resolved by SDS-PAGE and analyzed by immunoblotting.

Apoptosis assay

Suspended cells were treated with PND-1186, collected, stained for fluorescein (FITC)-conjugated annexin V binding (30 min), and analyzed within 1 h by flow cytometry. Quadrant gates were positioned based on cell autofluorescence (negative) staurosporine-treated (positive) controls. Apoptosis was calculated to be the percent of annexin V-positive cells.

Orthotopic breast cancer models

One million 4T1 or MDA-MB-231 cells in 10 μl PBS were injected into the T4 mammary fat pad of 8–10 week old mice using a Hamilton syringe. PND-1186 treatment (oral gavage or ad libitum) was initiated when the tumors were palpable (24–48 hr for 4T1 and after 12 days for MDA-MB-231). Tumors were measured every 3–4 days with digital vernier calipers and tumor volume (mm^3) was calculated using the formula: $V=axb^2/2$ (a=length, mm; b=width, mm). Body weight was measured weekly to assess toxicity. Lungs, spleen, and primary tumors were surgically removed and weighed. Tumors sections were homogenized in protein lysis buffer for immunoblotting or placed in Optimal Cutting Temperature (OCT) compound (Tissue Tek), frozen in liquid nitrogen, thin sectioned (7 μM) using a cryostat (Leica 3050S), and mounted onto glass slides.

For 4T1 tumor metastasis analyses, lungs were rinsed in PBS, dorsal and ventral fluorescent images acquired using the OV100 Small Animal Imaging System (Olympus). For all images, a common threshold for mCherry fluorescence was set and lung metastatic burden was calculated by determining the average integrated pixel density for micro-tumors present in each lung using Image J software. Metastatic tumor burden (number of metastatic lesion or mean pixel volume) was determined and groups (Negligible, Moderate, and High) were separated based upon numbers distribution. After imaging, lungs were fixed in Bouin's solution (Sigma), paraffin embedded, sectioned, and stained with hematoxylin and eosin (H&E) for histological evaluation. Images were acquired using a differential interference contrast-equipped Olympus IX81 inverted microscope and an Olympus DP71 digital color camera using Slidebook (v5.0) software. For MDA-MB-231 tumor metastasis studies, lungs were inflated by intratracheal injection of a 1:1 solution of OCT in sterile water using a 25 guage needle. Lungs were resected, embedded in OCT, and frozen in liquid nitrogen. Average number of lung metastases per lobe was determined by enumerating lung lesions in H&E sections (n=11 lobes for sucrose and n=13 lobes for PND-1186).

Experimental Metastasis Assay

Twelve week old nude mice were administered 150 mg/kg PND-1186 or water (vehicle) p.o. at 14 and 2 hours prior to the i.v. (via tail vein) injection of 0.5 million (in 100 μl PBS) MDA-MB-231 cells stably-expressing mCherry fluorescent protein. To determine experimental metastasis burden, lungs were removed 1 and 6 h post cell injection, rinsed in PBS, and dorsal plus ventral fluorescent images acquired using OV100 imaging. A common threshold for mCherry fluorescence was set for all images and the total fluorescent lung area was calculated using Image J.

Statistical Methods

Significant difference between groups was determined using one-way ANOVA with Tukey post hoc. Differences between pairs of data were determined using an unpaired two-tailed student's t-test or a two-tailed Mann-Whitney test. Differences between metastasis incidences were determined using a two-tailed Fisher's exact test. All statistical analyses were performed using GraphPad Prism (version 5.0b, GraphPad Software, San Diego CA). p-values of < 0.05 were considered significant.

Supplementary Material

Refer to Web version on PubMed Central for supplementary material.

Acknowledgments

We appreciate administrative assistance from Susie Morris and we thank Nichol Miller for critical review. Alok Tomar was supported by an American Heart Association Fellowship (0825166F). J. O. Nam was supported by a Korean Research Foundation fellowship (KRF-2008-357-E00007). This work was supported in part by Poniard funds and by NIH grants to D. Stupack (CA107263) and D. Schlaepfer (CA102310). D. Schlaepfer is an Established Investigator of the AHA (0540115N).

Abbreviations

ANOVA	analysis of variance
AUC(0-inf)	area under the plasma concentration-time curve from time zero to infinity
b.i.d	twice-daily
Cl	systemic clearance

C_{max}	the observed maximum plasma concentration after i.p. or p.o. dosing
ELISA	enzyme-linked immunosorbent assay
%F	bioavailability
FACS	fluorescence-activated cell sorting
FAK	focal adhesion kinase
FBS	fetal bovine serum
FITC	fluorescein isothiocyanate
HPLC	High-Performance Liquid Chromatography
IC_{50}	50% inhibitory concentration
IL-6	Interleukin-6
i.p.	intraperitoneal
i.v.	intravenous
MS/MS	Mass Spectrometry/Mass Spectrometry
OCT	optimal cutting temperature compound
p130Cas	130 kDa Crk-associated substrate
PBS	phosphate-buffered saline
PD	pharmacodynamics
PEG400	polyethylene glycol 400
p.o.	oral
PK	pharmacokinetics
SCID	severe combined immunodeficiency
SD	standard deviation
SDS-PAGE	sodium dodecyl sulfate polyacrylamide gel electrophoresis
SEM	standard error of the mean
$t_{1/2}$	log linear terminal half life
TNFα	tumor necrosis factor α
T_{MAX}	the time to reach C_{MAX} after i.p. or p.o. dosing
TUNEL	deoxynucleotidyl transferase dUTP nick end labeling
V_d	volume of distribution

References

1. Nicolini A, Giardino R, Carpi A, Ferrari P, Anselmi L, Colosimo S, et al. Metastatic breast cancer: an updating. Biomed Pharmacother. 2006; 60:548–556. [PubMed: 16950593]
2. Weigelt B, Peterse JL, van 't Veer LJ. Breast cancer metastasis: markers and models. Nat Rev Cancer. 2005; 5:591–602. [PubMed: 16056258]
3. White DE, Muller WJ. Multifaceted roles of integrins in breast cancer metastasis. J Mammary Gland Biol Neoplasia. 2007; 12:135–142. [PubMed: 17602286]
4. Schlaepfer DD, Hauck CR, Sieg DJ. Signaling through focal adhesion kinase. Prog Biophys Mol Biol. 1999; 71:435–478. [PubMed: 10354709]

5. Mitra SK, Hanson DA, Schlaepfer DD. Focal adhesion kinase: in command and control of cell motility. Nat Rev Mol Cell Biol. 2005; 6:56–68. [PubMed: 15688067]
6. Cance WG, Harris JE, Iacocca MV, Roche E, Yang X, Chang J, et al. Immunohistochemical analyses of focal adhesion kinase expression in benign and malignant human breast and colon tissues: correlation with preinvasive and invasive phenotypes. Clin Cancer Res. 2000; 6:2417–2423. [PubMed: 10873094]
7. Owens LV, Xu LH, Craven RJ, Dent GA, Weiner TM, Kornberg L, et al. Overexpression of the focal adhesion kinase (p125FAK) in invasive human tumors. Cancer Res. 1995; 55:2752–2755. [PubMed: 7796399]
8. Su GH, Song JJ, Repasky EA, Schutte M, Kern SE. Mutation rate of MAP2K4/MKK4 in breast carcinoma. Hum Mutat. 2002; 19:81. [PubMed: 11754110]
9. Watermann DO, Gabriel B, Jager M, Orlowska-Volk M, Hasenburg A, zur Hausen A, et al. Specific induction of pp125 focal adhesion kinase in human breast cancer. Br J Cancer. 2005; 93:694–698. [PubMed: 16136050]
10. Pylayeva Y, Gillen KM, Gerald W, Beggs HE, Reichardt LF, Giancotti FG. Ras- and PI3K-dependent breast tumorigenesis in mice and humans requires focal adhesion kinase signaling. J Clin Invest. 2009; 119:252–266. [PubMed: 19147981]
11. Agochiya M, Brunton VG, Owens DW, Parkinson EK, Paraskeva C, Keith WN, et al. Increased dosage and amplification of the focal adhesion kinase gene in human cancer cells. Oncogene. 1999; 18:5646–5653. [PubMed: 10523844]
12. Lark AL, Livasy CA, Dressler L, Moore DT, Millikan RC, Geradts J, et al. High focal adhesion kinase expression in invasive breast carcinomas is associated with an aggressive phenotype. Mod Pathol. 2005; 18:1289–1294. [PubMed: 15861214]
13. Lightfoot HM, Lark A, Livasy CA, Moore DT, Cowan D, Dressler L, et al. Upregulation of focal adhesion kinase (FAK) expression in ductal carcinoma in situ (DCIS) is an early event in breast tumorigenesis. Breast Cancer Res Treat. 2004; 88:109–116. [PubMed: 15564794]
14. Oktay MH, Oktay K, Hamele-Bena D, Buyuk A, Koss LG. Focal adhesion kinase as a marker of malignant phenotype in breast and cervical carcinomas. Hum Pathol. 2003; 34:240–245. [PubMed: 12673558]
15. Zouq NK, Keeble JA, Lindsay J, Valentijn AJ, Zhang L, Mills D, et al. FAK engages multiple pathways to maintain survival of fibroblasts and epithelia: differential roles for paxillin and p130Cas. J Cell Sci. 2009; 122:357–367. [PubMed: 19126677]
16. Mitra SK, Mikolon D, Molina JE, Hsia DA, Hanson DA, Chi A, et al. Intrinsic FAK activity and Y925 phosphorylation facilitate an angiogenic switch in tumors. Oncogene. 2006; 25:5969–5984. [PubMed: 16682956]
17. Lahlou H, Sanguin-Gendreau V, Zuo D, Cardiff RD, McLean GW, Frame MC, et al. Mammary epithelial-specific disruption of the focal adhesion kinase blocks mammary tumor progression. Proc Natl Acad Sci U S A. 2007; 104:20302–20307. [PubMed: 18056629]
18. Luo M, Fan H, Nagy T, Wei H, Wang C, Liu S, et al. Mammary epithelial-specific ablation of the focal adhesion kinase suppresses mammary tumorigenesis by affecting mammary cancer stem/progenitor cells. Cancer Res. 2009; 69:466–474. [PubMed: 19147559]
19. Hsia DA, Mitra SK, Hauck CR, Streblow DN, Nelson JA, Ilic D, et al. Differential regulation of cell motility and invasion by FAK. J Cell Biol. 2003; 160:753–767. [PubMed: 12615911]
20. Benlimame N, He Q, Jie S, Xiao D, Xu YJ, Loignon M, et al. FAK signaling is critical for ErbB-2/ErbB-3 receptor cooperation for oncogenic transformation and invasion. J Cell Biol. 2005; 171:505–516. [PubMed: 16275754]
21. Behmoaram E, Bijian K, Jie S, Xu Y, Darnel A, Bismar TA, et al. Focal adhesion kinase-related proline-rich tyrosine kinase 2 and focal adhesion kinase are co-overexpressed in early-stage and invasive ErbB-2-positive breast cancer and cooperate for breast cancer cell tumorigenesis and invasiveness. Am J Pathol. 2008; 173:1540–1550. [PubMed: 18832579]
22. Mitra SK, Lim ST, Chi A, Schlaepfer DD. Intrinsic focal adhesion kinase activity controls orthotopic breast carcinoma metastasis via the regulation of urokinase plasminogen activator expression in a syngeneic tumor model. Oncogene. 2006; 25:4429–4440. [PubMed: 16547501]

23. van Nimwegen MJ, Verkoeijen S, van Buren L, Burg D, van de Water B. Requirement for focal adhesion kinase in the early phase of mammary adenocarcinoma lung metastasis formation. Cancer Res. 2005; 65:4698–4706. [PubMed: 15930288]
24. Shibue T, Weinberg RA. Integrin beta1-focal adhesion kinase signaling directs the proliferation of metastatic cancer cells disseminated in the lungs. Proc Natl Acad Sci U S A. 2009; 106:10290–10295. [PubMed: 19502425]
25. Slack-Davis JK, Martin KH, Tilghman RW, Iwanicki M, Ung EJ, Autry C, et al. Cellular characterization of a novel focal adhesion kinase inhibitor. J Biol Chem. 2007; 282:14845–14852. [PubMed: 17395594]
26. Roberts WG, Ung E, Whalen P, Cooper B, Hulford C, Autry C, et al. Antitumor activity and pharmacology of a selective focal adhesion kinase inhibitor, PF-562,271. Cancer Res. 2008; 68:1935–1944. [PubMed: 18339875]
27. Shi Q, Hjelmeland AB, Keir ST, Song L, Wickman S, Jackson D, et al. A novel low-molecular weight inhibitor of focal adhesion kinase, TAE226, inhibits glioma growth. Mol Carcinog. 2007; 46:488–496. [PubMed: 17219439]
28. Liu TJ, LaFortune T, Honda T, Ohmori O, Hatakeyama S, Meyer T, et al. Inhibition of both focal adhesion kinase and insulin-like growth factor-I receptor kinase suppresses glioma proliferation in vitro and in vivo. Mol Cancer Ther. 2007; 6:1357–1367. [PubMed: 17431114]
29. Halder J, Lin YG, Merritt WM, Spannuth WA, Nick AM, Honda T, et al. Therapeutic efficacy of a novel focal adhesion kinase inhibitor TAE226 in ovarian carcinoma. Cancer Res. 2007; 67:10976–10983. [PubMed: 18006843]
30. Slack-Davis JK, Hershey ED, Theodorescu D, Frierson HF, Parsons JT. Differential requirement for focal adhesion kinase signaling in cancer progression in the transgenic adenocarcinoma of mouse prostate model. Mol Cancer Ther. 2009; 8:2470–2477. [PubMed: 19671741]
31. Parsons JT, Slack-Davis J, Tilghman R, Roberts WG. Focal adhesion kinase: targeting adhesion signaling pathways for therapeutic intervention. Clin Cancer Res. 2008; 14:627–632. [PubMed: 18245520]
32. Tanjoni I, Walsh C, Uryu S, Nam JO, Mielgo A, Tomar A, et al. PND-1186 FAK inhibitor selectively promotes tumor cell apoptosis in three-dimensional environments. Cancer Biology & Therapy, Submitted. 2009
33. Heppner GH, Miller FR, Shekhar PM. Nontransgenic models of breast cancer. Breast Cancer Res. 2000; 2:331–334. [PubMed: 11250725]
34. Coussens LM, Werb Z. Inflammation and cancer. Nature. 2002; 420:860–867. [PubMed: 12490959]
35. Colotta F, Allavena P, Sica A, Garlanda C, Mantovani A. Cancer-related inflammation, the seventh hallmark of cancer: links to genetic instability. Carcinogenesis. 2009; 30:1073–1081. [PubMed: 19468060]
36. DeNardo DG, Coussens LM. Inflammation and breast cancer. Balancing immune response: crosstalk between adaptive and innate immune cells during breast cancer progression. Breast Cancer Res. 2007; 9:212. [PubMed: 17705880]
37. Dupre SA, Hunter KW Jr. Murine mammary carcinoma 4T1 induces a leukemoid reaction with splenomegaly: Association with tumor-derived growth factors. Exp Mol Pathol. 2006; 82:12–24. [PubMed: 16919266]
38. Hodge DR, Hurt EM, Farrar WL. The role of IL-6 and STAT3 in inflammation and cancer. Eur J Cancer. 2005; 41:2502–2512. [PubMed: 16199153]
39. Aslakson CJ, Miller FR. Selective events in the metastatic process defined by analysis of the sequential dissemination of subpopulations of a mouse mammary tumor. Cancer Res. 1992; 52:1399–1405. [PubMed: 1540948]
40. Hollestelle A, Elstrodt F, Nagel JH, Kallemeijn WW, Schutte M. Phosphatidylinositol-3-OH kinase or RAS pathway mutations in human breast cancer cell lines. Mol Cancer Res. 2007; 5:195–201. [PubMed: 17314276]
41. Chiang AC, Massague J. Molecular basis of metastasis. N Engl J Med. 2008; 359:2814–2823. [PubMed: 19109576]

42. Provenzano PP, Inman DR, Eliceiri KW, Beggs HE, Keely PJ. Mammary epithelial-specific disruption of focal adhesion kinase retards tumor formation and metastasis in a transgenic mouse model of human breast cancer. Am J Pathol. 2008; 173:1551–1565. [PubMed: 18845837]
43. Mitra SK, Schlaepfer DD. Integrin-regulated FAK-Src signaling in normal and cancer cells. Curr Opin Cell Biol. 2006; 18:516–523. [PubMed: 16919435]
44. Lim S-T, Mikolon D, Stupack DG, Schlaepfer DD. FERM control of FAK function: Implications for cancer therapy. Cell Cycle. 2008; 7:2306–2314. [PubMed: 18677107]
45. Zheng Y, Xia Y, Hawke D, Halle M, Tremblay ML, Gao X, et al. FAK phosphorylation by ERK primes ras-induced tyrosine dephosphorylation of FAK mediated by PIN1 and PTP-PEST. Mol Cell. 2009; 35:11–25. [PubMed: 19595712]
46. Zhao J, Guan JL. Signal transduction by focal adhesion kinase in cancer. Cancer Metastasis Rev. 2009; 28:35–49. [PubMed: 19169797]
47. DeNardo DG, Johansson M, Coussens LM. Immune cells as mediators of solid tumor metastasis. Cancer Metastasis Rev. 2008; 27:11–18. [PubMed: 18066650]
48. Salgado R, Junius S, Benoy I, Van Dam P, Vermeulen P, Van Marck E, et al. Circulating interleukin-6 predicts survival in patients with metastatic breast cancer. Int J Cancer. 2003; 103:642–646. [PubMed: 12494472]
49. Schlaepfer DD, Hou S, Lim ST, Tomar A, Yu H, Lim Y, et al. Tumor necrosis factor-alpha stimulates focal adhesion kinase activity required for mitogen-activated kinase-associated interleukin 6 expression. J Biol Chem. 2007; 282:17450–17459. [PubMed: 17438336]
50. Earley S, Plopper GE. Phosphorylation of focal adhesion kinase promotes extravasation of breast cancer cells. Biochem Biophys Res Commun. 2008; 366:476–482. [PubMed: 18073135]

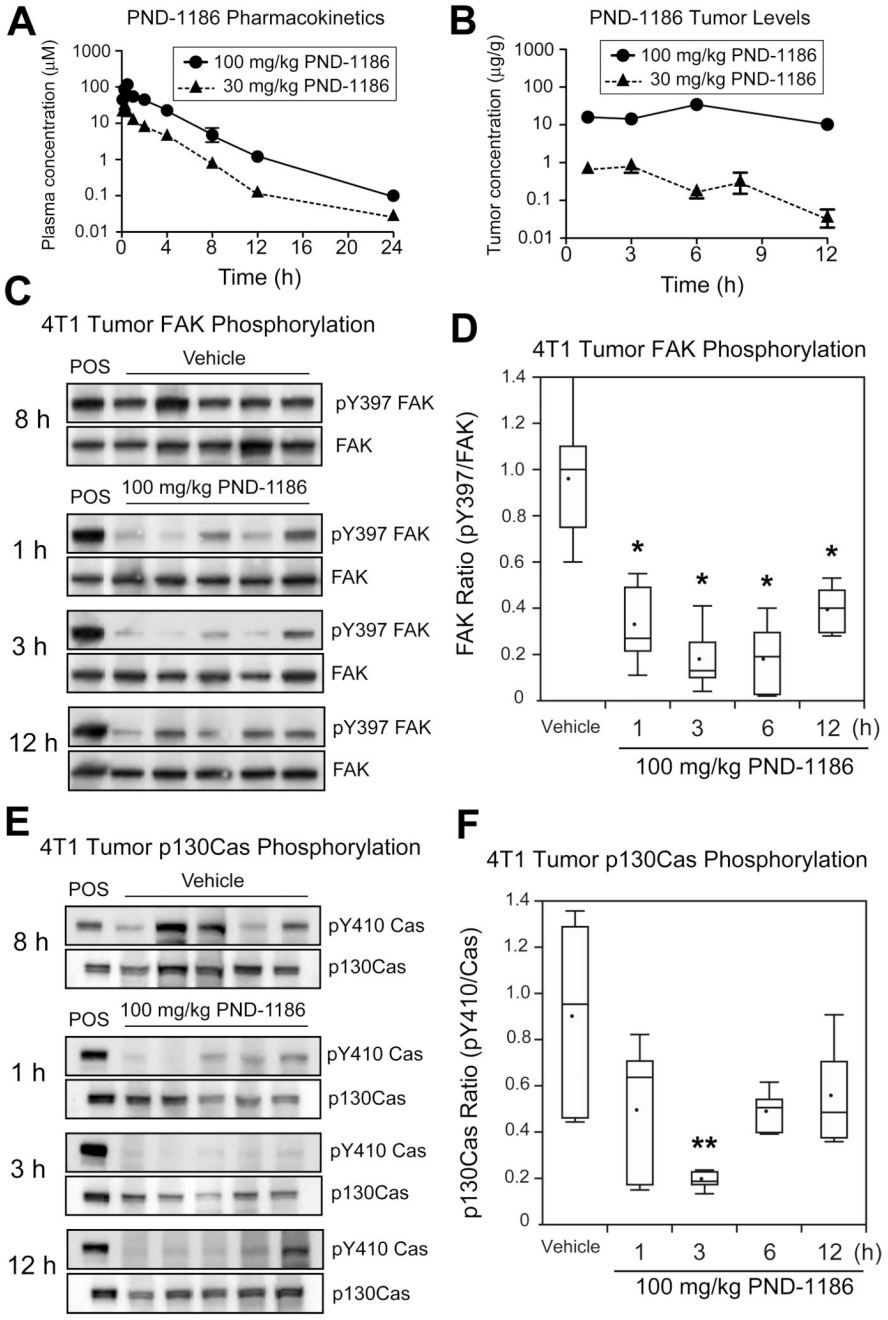

Figure 1. PND-1186 pharmacokinetic profile and inhibition of tumor-associated FAK and p130Cas tyrosine phosphorylation

A single single intraperitoneal (i.p.) dose of 30 or 100 mg/kg PND-1186 was administered to mice and drug levels in (A) plasma (n=3 per time point) and (B) tumor samples (n=5 per time point) were determined by HPLC and mass spectroscopy at the times indicated. Error bars are +/− SD. (C–F) Subcutaneously grown 4T1 tumors from mice treated with a single 100 mg/kg PND-1186 i.p. dose were collected and lysed at the times indicated (n=5 tumors per time point). (C) Representative immunoblots for phosphorylated FAK Tyr-397 (pY397 FAK) and total FAK in vehicle and PND-1186-treated tumors. Lane 1 (POS) is a positive control of 4T1 cell lysate. (D) Box-whisker plots of FAK pY397 to total FAK ratio in

PND-1186 treated tumors over time. (E) Representative immunoblots for phosphorylated p130Cas Tyr-410 (pY410 Cas) and total p130Cas in vehicle and PND-1186-treated tumors. Lane 1 (POS) is a positive control of 4T1 cell lysate. (F) Box-whisker plots of p130Cas pY410 to total p130Cas ratio in PND-1186 treated tumors over time. Box-and-whisker diagrams show the distribution of the data: square, mean; bottom line, 25^{th} percentile; middle line, median; top line, 75^{th} percentile; and whiskers, 5^{th} or 95^{th} percentiles. Significant differences between groups were ascertained using ANOVA followed by the Tukey post hoc test, (* $p < 0.0001$, ** $p = 0.008$).

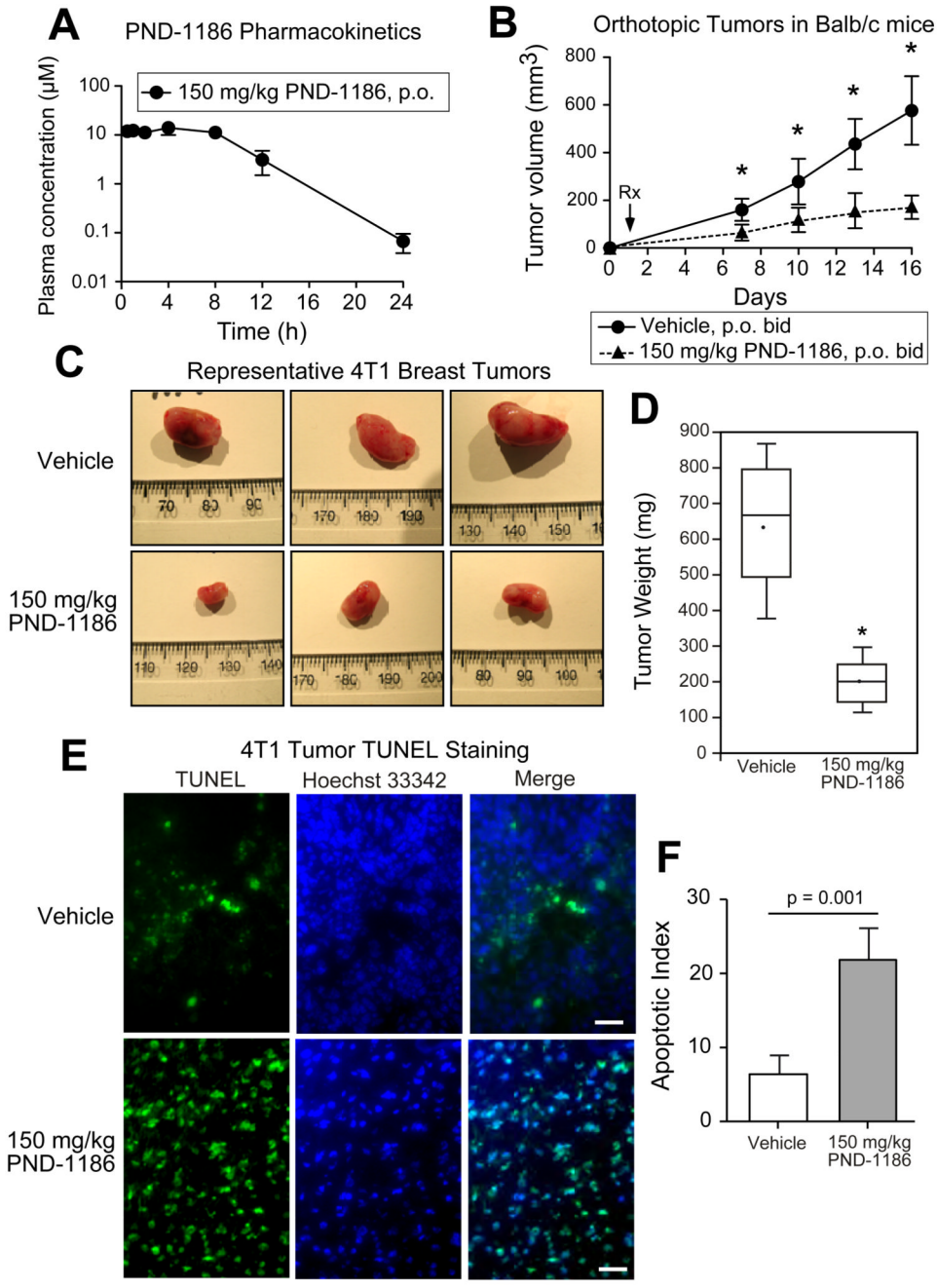

Figure 2. Oral PND-1186 administration inhibits orthotopic 4T1 breast carcinoma tumor growth associated with increased apoptosis

(A) A single oral (p.o.) dose of PND-1186 at 150 mg/kg was administered to mice and plasma drug levels (n=3 per time point) were determined by HPLC and mass spectroscopy at the times indicated. Error bars are +/− SD. (B) mCherry-4T1 tumor cells were implanted in the fat pad of BALB/c mice. Mice were administered vehicle (water) or 150 mg/kg PND-1186 p.o. twice-daily (b.i.d.) for 15 days (n=12 per group). Treatment began 24 hours after cell implantation. Tumor growth was significantly inhibited by PND-1186 treatment at Day 7 as determined by caliper measurements and error is +/− SD. (C) Representative 4T1 tumors from vehicle and PND-1186-treated mice. (D) Average final 4T1 tumor weight from

vehicle and PND-1186-treated mice (n=12 per group). (E) Representative images of TUNEL stained 4T1 tumor sections from vehicle and PND-1186-treated mice. Green is FITC-labeled TUNEL and blue is DNA stain (Hoechst 33342). Scale bar is 200 μm. (F) Quantification of 4T1 tumor TUNEL staining. Apoptotic index is defined as percent of total field FITC stain, bars are mean +/− SEM. Independent images analyzed: Vehicle=144 and PND-1186=77. Box-and-whisker diagrams show the distribution of the data: square, mean; bottom line, 25th percentile; middle line, median; top line, 75th percentile; and whiskers, 5th or 95th percentiles. Significant differences were ascertained using an unpaired two-tailed student's t-test, (* $p < 0.0001$).

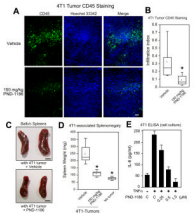

Figure 3. PND-1186 reduces inflammatory cell infiltration in primary 4T1 tumors, tumor-associated splenomegaly, and inhibits TNF*α*–stimulated IL-6 secretion from 4T1 cells in culture

Orthotopic mCherry-4T1 tumors in Balb/c mice were treated with vehicle (water) or 150 mg/kg PND-1186 as described in Figure 2. (A) Primary tumors were sectioned and stained for anti-CD45 macrophage-associated marker (FITC, green) and with Hoechst 33342 (blue). Representative images are shown. Scale bar is 1 mm. (B) Quantification CD45 stained sections using Image J and the Infiltration index is defined as the average area occupied by FITC staining (mm^2). Independent images analyzed: Vehicle=169 and PND-1186=52. (C) Representative spleen images from mice treated with vehicle (water) or 150 mg/kg PND-1186 p.o. b.i.d. Scale bar is 0.5 cm. (D) Average spleen weight from non-tumor-bearing mice or tumor-bearing mice treated with vehicle (water) or 150 mg/kg PND-1186 p.o. b.i.d. (n=12 per group). (E) 4T1 cells were pretreated for 1 h with DMSO (C, control) or the indicated concentration of PND-1186. Tumor necrosis factor-α (TNFα) was added (10 ng/ml) for 24 h and IL-6 levels in conditioned media measured using anti-mouse IL-6 ELISA. Results represent two independent experiments with triplicate points and error bars are +/− SD. Box-and-whisker diagrams show the distribution of the data: square, mean; bottom line, 25^{th} percentile; middle line, median; top line, 75^{th} percentile; and whiskers, 5^{th} or 95^{th} percentiles. Infiltration index significant difference was ascertained using an unpaired two-tailed student's t-test and spleen weight difference was determined using ANOVA followed by the Tukey post hoc test, (* $p < 0.0001$).

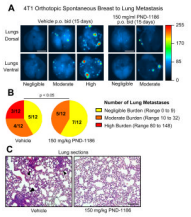

Figure 4. PND-1186 prevents spontaneous 4T1 breast to lung tumor metastasis

Orthotopic mCherry-4T1 tumors in Balb/c mice were treated with vehicle (water) or 150 mg/kg PND-1186 as described in Figure 2. (A) After 16 days, lungs were examined *ex vivo* for mCherry fluorescence and shown are representative dorsal and ventral lung images from vehicle or 150 mg/kg PND-1186 treated mice. Images have been heat mapped (scale at right) to highlight pixel fluorescence intensity. Scale is 0.5 cm. (B) Distribution of metastasis incidence. Lung metastatic lesions were enumerated by analysis of dorsal/ventral images thresholded by Image J software. Fractions represent the number of lungs with negligible (yellow), moderate (orange) or high (red) burden over total number analyzed. Data is total mCherry metastatic lesions per lung lobe (n=12 per group, no values between 33 and 79). (C) Representative H&E stained medial lung sections showing 4T1 metastatic lesions (arrows) in vehicle control mice. Scale bar is 0.2 mm. Metastasis incidence significance was determined using the Fisher's exact test.

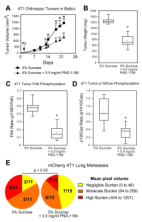

Figure 5. Low-level *ad libitum* PND-1186 administration inhibits FAK-p130Cas tyrosine phosphorylation and 4T1 tumor growth-metastasis

mCherry-4T1 tumor cells were implanted in the fat pad of BALB/c mice. After 48 h, mice were provided 5% sucrose (control) or 0.5 mg/kg PND-1186 in 5% sucrose in lieu of drinking water. Administration was *ad libitum*. (A) 0.5 mg/ml PND-1186 significantly inhibited orthotopic 4T1 tumor growth by Day 13 (†, $p<0.01$) as determined by caliper measurements and error is +/− SD. (B) Average final 4T1 tumor weight at Day 22 (n=11 for control and n=15 for PND-1186). (C) Box-whisker plot ratio of FAK pY397 to total FAK in 5% sucrose or 0.5 mg/ml PND-1186 treated tumors. (D) Box-whisker plot ratio of p130Cas pY410 to total p130Cas in 5% sucrose or 0.5 mg/ml PND-1186 treated tumors (C and D) n=11 for sucrose control and n=15 for PND-1186. (E) Distribution of metastasis incidence. Lung metastatic lesions were quantified using Image J by calculating the average pixel volume (integrated density) of thresholded images. Fractions represent the number of lungs with negligible (yellow), moderate (orange) or high (red) burden over total number analyzed. Data is mean pixel volume +/− SEM. Box-and-whisker diagrams show the distribution of the data: square, mean; bottom line, 25th percentile; middle line, median; top line, 75th percentile; and whiskers, 5th or 95th percentiles. Significant differences between pairs of data were ascertained using an unpaired two-tailed student's t-test. Significant differences between metastasis incidences were determined using Fisher's exact test, (†, $p<0.01$, * $p < 0.0001$).

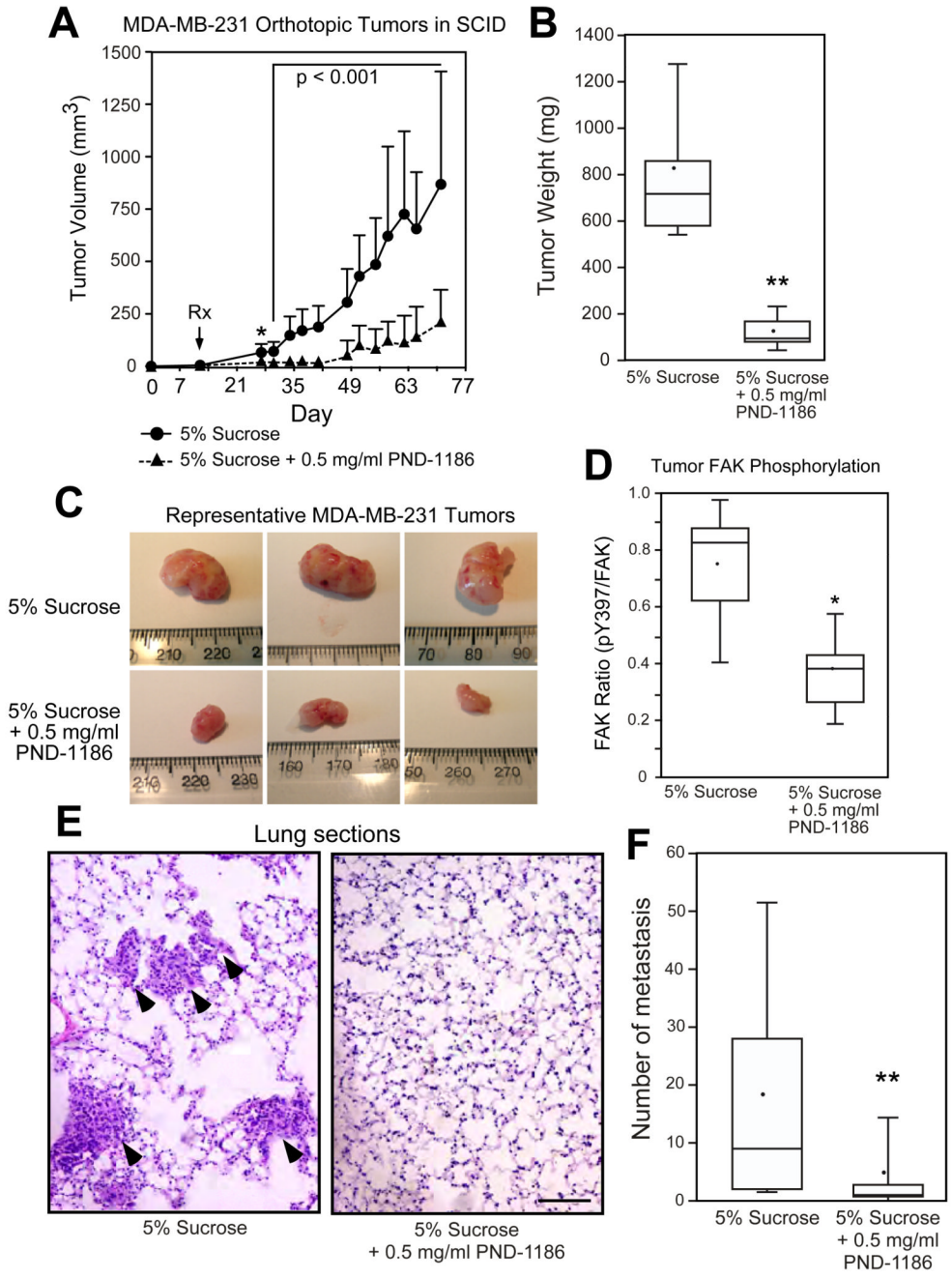

Figure 6. Low-level *ad libitum* PND-1186 administration inhibits orthotopic MDA-MB-231 tumor growth, FAK phosphorylation, and lung metastasis

MDA-MB-231 cells were implanted in the breast fat pad of SCID mice. After 12 days, mice were provided 5% sucrose (control) or 0.5 mg/kg PND-1186 in 5% sucrose in lieu of drinking water. Administration was *ad libitum*. (A) 0.5 mg/ml PND-1186 significantly inhibited orthotopic 4T1 tumor growth by Day 27 (*) as determined by caliper measurements and error is +/− SD. (B) Average final MDA-MB-231 tumor weight at Day 70 (n=11 for sucrose control and n=13 for PND-1186). (C) Representative images of MDA-MB-231 tumors from 5% sucrose (control) and 0.5 mg/ml PND-1186-treated mice. (D) Box-whisker plot ratio of FAK pY397 to total FAK in 5% sucrose or 0.5 mg/ml PND-1186

treated tumors (n=11 for sucrose control and n=13 for PND-1186). (E) Representative H&E stained medial lung sections showing MDA-MB-231 metastatic lesions (arrows) in control mice. Scale bar is 0.2 mm. (F) Average number of lung metastases per lobe was determined by enumerating lung lesions in H&E sections (n=11 lobes for sucrose and n=13 lobes for PND-1186). Box-and-whisker diagrams show the distribution of the data: square, mean; bottom line, 25^{th} percentile; middle line, median; top line, 75^{th} percentile; and whiskers, 5^{th} or 95^{th} percentiles. Significant differences between groups were ascertained using an unpaired two-tailed student's t-test and differences between metastasis number were determined using a Mann-Whitney test, (* $p < 0.05$, ** $p < 0.0001$).

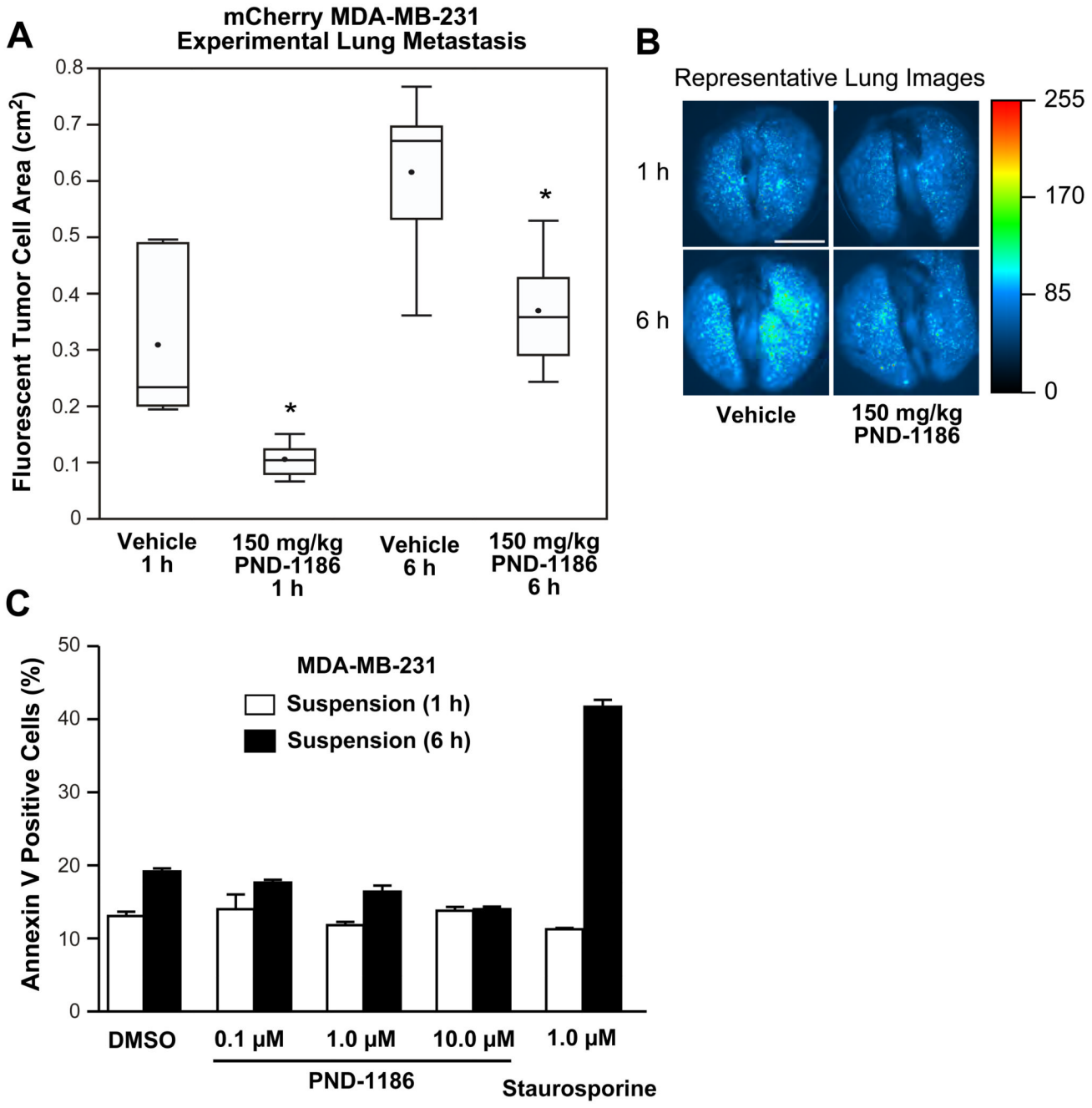

Figure 7. PND-1186 decreases lodging of fluorescent MDA-MB-231 cells in the lung

(A) Experimental metastasis plotted as the total fluorescent area of mCherry-expressing MDA-MB-231 cells present in mouse lungs at 1 and 6 h after i.v. tail vein injection (n=3 mice per group). Mice were treated with 150 mg/kg PND-1186 or water (vehicle) p.o. prior to tumor cell injection. (B) Representative dorsal fluorescent lung images from vehicle or 150 mg/kg PND-1186 treated mice were heat mapped (scale at right) to highlight pixel fluorescence intensity. Scale bar is 0.5 mm. Box-and-whisker plots show the distribution of the data: square, mean; bottom line, 25th percentile; middle line, median; top line, 75th percentile; and whiskers, 5th or 95th percentiles. Significant differences between groups were ascertained using one-way ANOVA followed by the Tukey post hoc test, (* $p < 0.05$).

(C) Flow cytometry was used to determine the percentage of annexin V-positive staining from suspended MDA-MB-231 cells treated for 1 h or 6 h with DMSO or the indicated amount of PND-1186. Staurosporine (1 μM) treatment was used as a postive control.

Table 1

PND-1186 pharmacokinetic (PK) parameters after intravenous (i.v.), intraperitoneal (i.p.), oral (p.o.), and *ad libitum* dosing in mice.

Dose	C_{MAX} (μM)	T_{MAX} (h)	C_{SS} (μM)	$t_{1/2}$ (h)	AUC(0-inf) (ng·h/mL)	Vd (ml/kg)	Cl (ml/h/kg)	%F
PND-1186 2 mg/kg i.v.	-	-	-	1.72	6,960	714	287	-
PND-1186 30 mg/kg i.p.	34.76	0.25	-	2.27	32,500	-	-	31.1
PND-1186 100 mg/kg i.p.	117.10	0.50	-	2.65	147,000	-	-	42.2
PND-1186 150 mg/kg p.o.	13.98	4.00	-	2.15	77,400	-	-	14.8
PND-1186 0.5 mg/kg *ad libitum*	-	-	1.16	-	13.1	-	-	-

PK parameters listed include the observed maximum plasma concentration (C_{max}) and time to maximum concentration (T_{max}) after i.p. or p.o. dosing, area under the plasma concentration-time curve from time zero to infinity AUC(0-inf), volume of distribution (V_d), systemic clearance (Cl), log linear terminal half life ($t_{1/2}$,) and the bioavailability (%F). PK analyses were performed by non-compartmental analysis using model 200 for i.p. and p.o. and model 201 for the i.v. in WinNonlin Professional 4.1 (Pharsight Corp., Mountain View, CA).